# Numerical Simulation of Paced Electrogram Fractionation: Relating Clinical Observations to Changes in Fibrosis and Action Potential Duration

IAN TURNER, B.SC., D.PHIL.,* CHRISTOPHER L.-H. HUANG, M.D., SC.D.,† and RICHARD C. SAUMAREZ, PH.D., F.R.C.P.‡

From the *Papworth Hospital, †Physiological Laboratory, ‡Departments of Engineering and Medicine, University of Cambridge, United Kingdom

**Simulating Paced Electrogram Fractionation.** ***Introduction:*** **Paced electrogram fractionation analysis (PEFA) may identify a re-entrant substrate in patients at risk of ventricular fibrillation (VF) by detecting prolonged, fractionated ventricular electrograms ("fractionation") in response to premature extrastimuli. Numerical simulations of action potential (AP) propagation through human myocardium following such premature stimulation were performed to study the relationship between electrogram fractionation, fibrosis, and changes in AP currents.**

***Methods and Results:*** **Activation in a resistive monodomain 2 $cm^2$ sheet of myocardium containing nonconducting fibrous tissue was modeled using standard numerical methods for solutions of partial differential equations using the Priebe–Beukelmann (PB) AP equations. Myocardial fibrosis significantly influenced electrogram morphology. High densities of closely spaced fibrous septa caused functional block and altered propagation paths at short coupling intervals, and produced large increases in electrogram duration similar to those associated with increased risk of VF in clinical studies. Prolongation of the cardiac AP using the heart failure variant of the PB model further increased the amount of fractionation and thereby replicated clinical recordings more closely than did fibrosis alone. Increasing AP dispersion by a variable reduction in the potassium current $I_{Kr}$ simulated results seen in patients with the long QT syndrome with an abrupt increase in electrogram duration, while a uniform reduction in $I_{Kr}$ alone did not result in fractionated electrograms. In contrast, increases in cytosolic $Ca^{2+}$ and $Ca^{2+}$ buffering by troponin to simulate HCM had little effect on fractionation.**

***Conclusions:*** **These results relate the effects of fibrosis, AP abnormalities, and dispersion of AP duration to the characteristic electrograms recorded in patients at risk of sudden death.** *(J Cardiovasc Electrophysiol, Vol. 16, pp. 151-161, February 2005)*

*electrogram, fractionation, sudden death (cardiac), computer simulation, action potential model*

## Introduction

Ventricular fibrillation (VF) is initiated and sustained by a functional re-entrant substrate with continually changing regions of slow conduction and block.[1-3] This functional substrate is the consequence of myocardial fibrosis, gap junctions, and action potential (AP) abnormalities. However, its complexity and transient nature makes it difficult to detect in patients at risk of sudden cardiac death (SCD).[4-6] This problem led to the application of paced electrogram fractionation analysis (PEFA),[7-9] originally used to study patients specifically with hypertrophic cardiomyopathy (HCM), who are at increased risk of VF.

PEFA delivers a decremental pacing sequence to the ventricle and records electrograms from other ventricular sites to infer abnormal patterns of myocardial activation by analyzing changes in electrogram waveforms that were obtained in response to premature (S2) stimuli. PEFA uses the finding that normal propagation of the AP produces a single, biphasic deflection whereas the presence of abnormal, discontinuous and potentially reentrant propagation following an S2 stimulus produces multiple, delayed potentials in the recorded electrogram ("fractionation").[7] This hypothesis arose from early clinical PEFA studies that showed that control patients had electrograms that maintained a roughly constant waveform despite a reduction of the S1–S2 interval whereas patients who had survived, or subsequently developed, VF showed marked electrogram fractionation at reduced S1–S2 intervals.[7-9] These findings have been confirmed in a more recent study of 285 patients with a variety of noncoronary cardiac; disease[10] this demonstrated that fractionation was most pronounced in the 79 patients with a retrospective or subsequent history of VF and was significantly less pronounced in the remaining non-VF patients. Although the mechanism by which it occurs may be different in each disease, increased electrogram fractionation appears to be a general effect associated with a risk of SCD[10] in patients with HCM, dilated cardiomyopathy (DCM), idiopathic VF, and the long QT Syndrome (LQTS)

This work was supported in part by the British Heart Foundation.

Dr. Saumarez is the founder of Medilec, which manufactures equipment that was used to perform the clinical procedure mentioned in this study. Medilec is located in Cambridge, Cambridgeshire, England.

Address for correspondence: Dr. R.C. Saumarez, Department of Engineering, University of Cambridge, Cambridge, CB2 1PZ, UK. E-mail: rcs23@eng.cam.ac.uk

Received 4 September 2004; Revised manuscript received 26 August 2004; Accepted for publication 30 August 2004.

doi: 10.1046/j.1540-8167.2005.30490.x

and so suggests a means of risk stratification in these diseases. This article describes a numerical model for the PEFA phenomenon and thereby clarifies the relationship between electrogram fractionation and pathological changes in myocardial fibrosis and AP abnormalities that may create an arrhythmic substrate.

### *Paced Electrogram Fractionation Analysis*

Four bipolar electrode catheters are introduced into different locations within the right ventricle[7-9] and a pacing sequence is delivered from one electrode and electrograms are recorded from the remaining three. The sequence was devised in order to obtain a large number of responses to premature stimuli (S2) in a reasonable length of time and consists of a two-beat drive train (490 ms S1–S1 interval) followed by a premature stimulus. This cycle is repeated with the S1–S2 coupling interval being reduced from 450 ms down to 220 ms in 1-ms steps so giving 230 electrograms in response to extrastimuli per channel on each sequence.

The recordings are analyzed by detecting the individual potential deflections in the high-pass, zero-phase, filtered electrograms. The delay of each deflection following the stimulus is plotted against the coupling interval at which the electrogram was obtained to produce fractionation curves (Fig. 1). The curves are then characterized by two measures that are related to the risk of SCD, which were proposed on the basis of the first 37 patients with HCM, but have now been prospectively tested with over 285 patients.[10] The first is the increase in electrogram duration between baseline and the shortest S1–S2 interval (Δ Electrogram Duration, ΔED), which represents the capacity of the myocardium to generate slowed conduction, i.e., to act as an arrhythmic substrate. The second measure, the S1–S2 interval at which the absolute electrogram duration starts to prolong ($S1–S2_{delay}$), is thought to represent the likelihood of patients developing a substrate in response to arrhythmogenic triggers.

## Methods

### *Numerical Simulation of the Spread of Action Potentials*

The model was a standard, monodomain resistive network,[11-14] representing a single cell layer, in which the extracellular space was grounded, so removing variations in extracellular resistive connections between cells.[15] Fibrous tissue was represented as barrier 10 times the length and diameter of a cardiomyocyte with an infinite resistance (Fig. 2A), making extracellular currents unlikely to cause propagation across fibrous tissue, which was assumed to completely block activation.

Anisotropic propagation[13-15] was modeled by using an intracellular resistivity along the long axis of the cells (*y*-axis) of 500 Ω cm and 3500 Ω cm in the transverse direction.

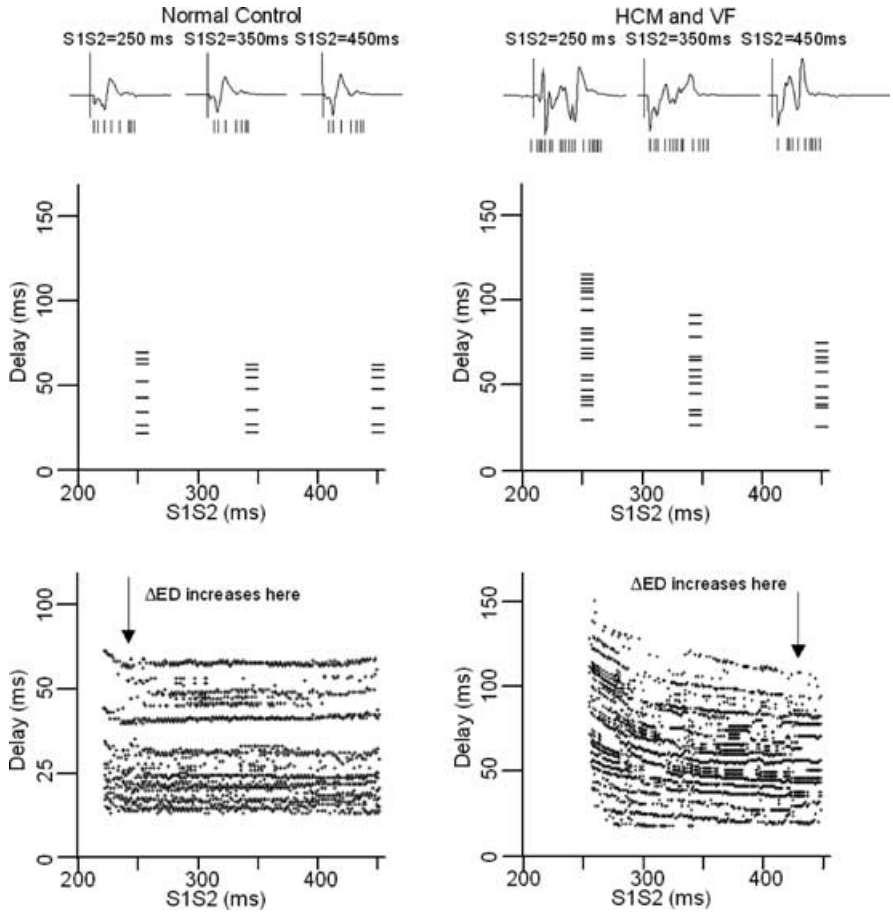


**Figure 1.** *The main steps in producing the electrogram fractionation curves. Electrograms at three different S1–S2 intervals are shown at the top. The delay of each detected peak is plotted for each of these S1–S2 intervals below this. The bottom traces show curves from a control and a patient with HCM and a history of VF and illustrate the electrogram prolongation and changes in activation sequence seen in VF patients.*

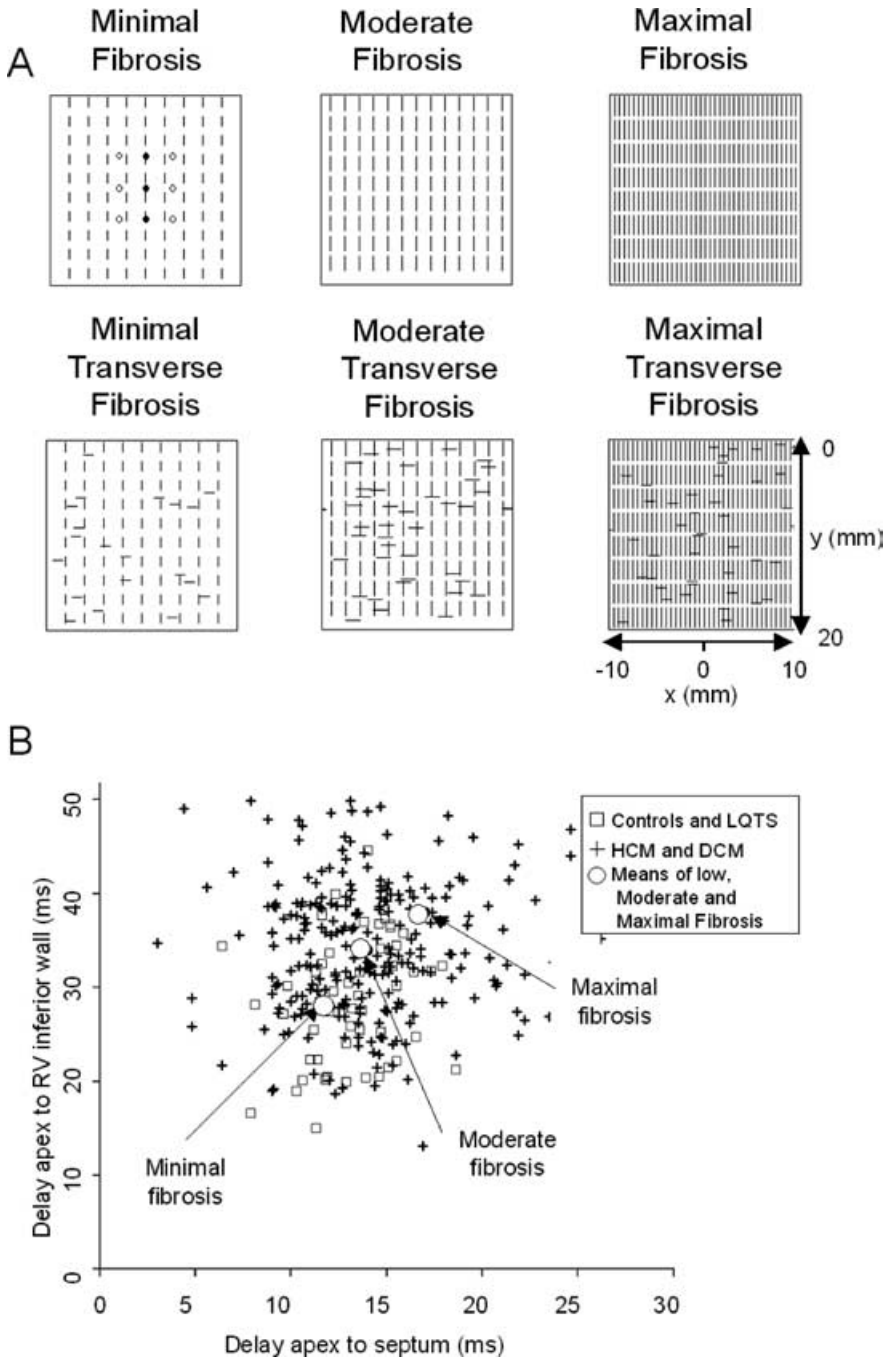


**Figure 2.** *(A) The distribution of RV septum and RV inferior wall delays following a drive beat stimulus. The squares represent controls and LQTS patients and the crosses represent HCM and DCM patients. The delays is obtained by band limited Fourier interpolation of the recorded signal. The theoretical delays for minimal, moderate, and severe fibrosis models are shown. (B) The patterns of fibrosis for the different types of tissue simulations. High-resistance fibrotic elements are shown in black. The sheets represent a 2 × 2 cm area, composed of 200 by 200 elements. The electrode positions are shown in the top left diagram.*

The tissue sheet was formed by an array of 201 by 201 elements, each 100 $\mu$m square, with defined AP properties and electrical resistance between its neighbors. The finite difference equations describing the transmembrane voltage in terms of the intercellular resistances, membrane capacitance, and ion currents, were solved using 10 $\mu$s steps using the alternate-direct-implicit (ADI) Crank-Nicholson method.[16] Sealed-edge (Neumann) boundary conditions[17] were used, and the initial conditions for the first beat of each simulation were defined by the gating variables, and transmembrane current and voltage for a cell after prolonged pacing at S1–S1 of 490 ms. Computation of the activation front with the assumed axial and transverse resistivities produced delays (stimulus to intrinsic deflection) between the apex and septum and apex and RV inferior wall, which were consistent with the delays seen in clinical studies (Fig. 2B) for different levels of fibrosis (Fig. 2A).

Bipolar electrograms were computed for electrodes placed over the sheet simulating the bipolar recordings used clinically. The electrodes formed bipolar pairs, one on the central

axis ($x = 0$) with poles at ($y = 7.5$ mm and $y = 12.5$ mm), and two *off-axis* ($x = \pm 2.5$ mm, $y = 7.5$ or 12.5 mm). These positions were far enough from the edge of the model to avoid discontinuities in the computed electrograms caused by the depolarizing wave front encountering the model boundaries.

### *Modeling the Action Potential*

The APs were modeled by the Priebe-Beuckelmann (PB) equations,[18] which describe human APs rather than those from small mammalian hearts[19] and can be modified to include the effects of heart failure. In HCM, myocytes are typically hypertrophied and have prolonged APs, similar to those in heart failure,[20,21] and were modeled using standard modifications of the PB[18] model, including increased $Na^+-Ca^{2+}$ exchanger activity, a slower diastolic decay in $Ca^{2+}$ transient, reduced $Na^+-K^+$ pump activity, and reduced inward rectifier currents. To simulate the abnormal $Ca^{2+}$ kinetics in HCM, the dissociation constant of $Ca^{2+}$ binding to troponin was increased twofold. The $Ca^{2+}$ uptake by the junctional sarcoplasmic reticulum (JSR) and longitudinal sarcoplasmic reticulum (LSR) was modified by a 15% decrease in calsequestrin binding and the calcium uptake current, $I_{Ca_{2+}\,up}$ was scaled between 0.0045 and 0.001 mmol/(L ms) to change cytosolic [$Ca^{2+}$], which was allowed to equilibrate at an increased level of 0.23 mmol.

### *Modeling Myocardial Fibrosis*

Mapping and simulation studies have shown that myocardial fibrosis creates tortuous paths around multiple, nonconducting obstacles, which leads to complex patterns of activation.[2,15,22,23] Fibrosis, usually arranged as septae that are parallel to the long axis of the myocyte,[2] may form the critical, slowly conducting part of re-entry circuits by slowing or producing a local block of transverse conduction and results in fractionated electrograms in nearby recording electrodes.[14,15,22] The septa are normally short, typically 0.5–1 mm, but may be increased to 3 mm in length in highly fibrotic tissue.[2,19,24] Longitudinal fibrosis, with septae parallel to the fiber axis, was modeled by three different, regular grids of lines of insulating, inexcitable elements (Fig. 2A). The pattern of fibrosis was determined by the length of the lines ($L$), the spacing between adjacent bundles ($S$), and the size of the gaps between the lines in the transverse direction ($G$). The three grids represented minimal fibrosis ($L = 1.0$ mm, $S = 2.0$ mm, $G = 1.0$ mm, area = 2.5%), moderate (L = 1.5 mm, S = 1.5 mm, G = 0.7 mm, area = 4.5%), or severe fibrosis (L = 2.0 mm, S = 1.0 mm, G = 0.5 mm, area = 16.5%). These values are consistent with reported values for normal tissue (0–2% fibrosis) or tissue from patients with documented VF (5–20%).[2,23,25,26] While the majority of the fibrosis in normal hearts, or in postinfarction scarring, is longitudinal, there is also some fibrous tissue transverse to the fiber axis and this is increased in HCM.[25,26] This was modeled by including more lines of transverse fibrosis, which were added in random positions on the HCM model to a maximum of 2% of the area of the sheet (Fig. 2).

### *Solution Method Used to Produce the Fractionation Curves*

The simulations modeled clinical recordings using the same S1–S2 intervals, electrode configuration, and signal processing. They were performed using a two-beat drive train followed by a premature S2 with a reduction of the S1–S2 interval from 450 to 300 ms in 5-ms steps. Stimulation was carried out at twice the current threshold over $5 \times 5$ elements at the middle of one edge ($x = 0$, $y = 0$). The simulated electrograms were computed by integration of the current field over the sheet and processed with a zero-phase high-pass filter (150 Hz, single pole) to emphasize small transient potentials and remove repolarization signals. Any potential that was above a fixed voltage threshold of 20 $\mu$V was detected (the clinical technique uses an adaptive threshold dependent on the signal noise) and the delay of each potential in the electrogram was plotted against the S1–S2 interval at which it was obtained to form the simulated fractionation curves.

The curves were then characterized by the increase in duration between an S1–S2 interval of 350 ms and the shortest S1–S2 interval, ($\Delta$ED) and the S1–S2 interval at which the delay of the last peak increased by more than 2 ms above baseline ($S1–S2_{delay}$).

## Results

### *Effects of Longitudinal Fibrosis*

Simulated electrograms and fractionation curves for electrodes on the central axis, and off-center, are shown in Figure 3 for the fibrosis-free sheet and the sheet with high levels of fibrosis (Fig. 4). The electrograms remain constant in simulations without fibrosis, becoming slightly wider and more delayed at short coupling intervals whereas there are large changes in electrogram duration and morphology at short S1–S2 intervals for the highly fibrotic sheet (Table 1), particularly in the transverse direction. The degree of fractionation increases with the amount of fibrosis present, especially at coupling intervals just above the effective refractory period (ERP) and is more pronounced for electrodes measuring transverse propagation, and is seen in a number of HCM VF patients.

### *The Effects of Transverse Fibrosis*

Random lines of transverse fibrosis were added to the sheets with longitudinal fibrosis and the simulations repeated. Five different patterns of random fibrosis were simulated for each pattern of longitudinal fibrosis. The $\Delta$ED and $S1–S2_{delay}$ measurements were averaged over the five examples for the different electrodes (Table 2) and the addition of transverse fibrosis led to a marked increase in electrogram fractionation at longer S1–S2 intervals. Again, this was particularly apparent for the bipolar electrode on the central axis of the sheet and in all cases the electrogram delay increased at long S1–S2 intervals. One random pattern of fibrosis (not included in Table 2) produced extremely large increases in fractionation, similar to that seen in some patients prior to development of VF,[7] and was able to support VF-like reentry (Fig. 4).

### *Effects of Abnormal APs*

The simulations were repeated using the heart failure AP to represent the effects of HCM or DCM on cellular electrophysiology using sheets with moderate fibrosis. Typical results are shown in Figure 5. The heart failure AP shifted the curve to the right (i.e., changes occurred at longer S1–S2 intervals) due to the longer refractory period predicted by the PB model. The average $\Delta$ED and $S1–S2_{delay}$ values (and 95%

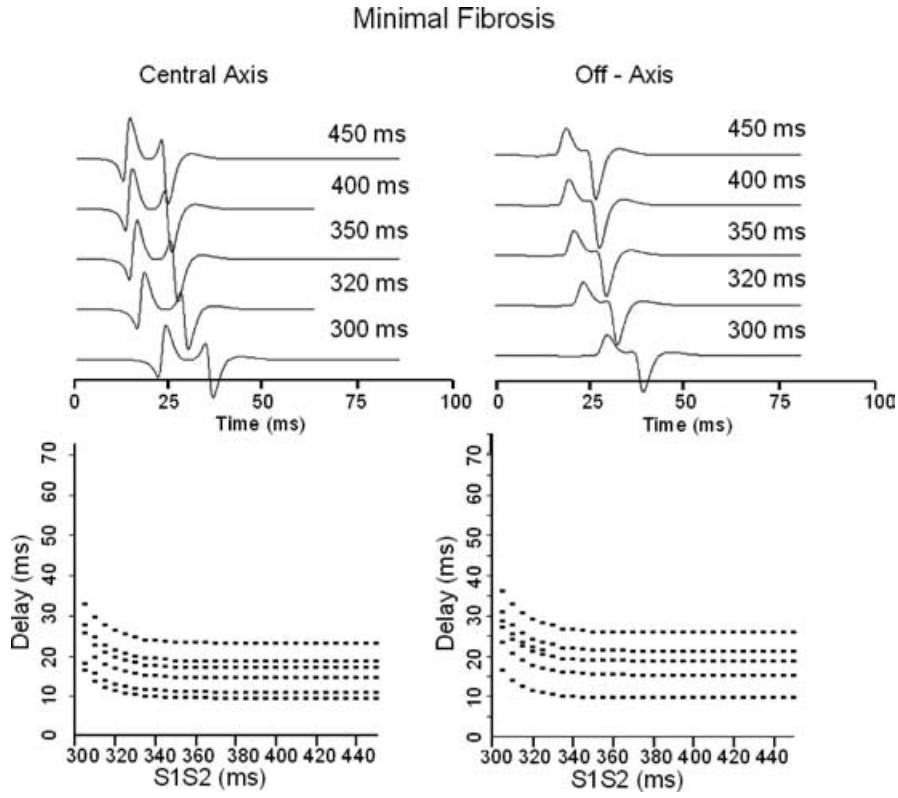


**Figure 3.** *The simulated electrograms for electrodes on and off the central axis are shown at different S1–S2 intervals. These are for the tissues with minimal fibrosis. The corresponding fractionation curves for the simulations, after peak detection and plotting, are shown below.*

confidence limits) for the central axis electrode were 9.6 (± 1.2) ms and 360 (± 8) ms, respectively, while the off-axis electrodes had $\Delta ED = 14.9$ (± 2.7) ms and $S1–S2_{delay} = 380$ (±9) ms, all significantly different ($P < 0.05$) from those with the same sheets but normal APs (Table 2).

Using the simulations based on the heart failure AP, dispersion was modeled by setting the slow potassium current, $I_{Ks}$ to be 50–100% of the normal level in a random distribution over the entire sheet resulting in a 20% increase in maximum AP duration. The fractionation curve shows a significant change in electrogram morphology at short coupling intervals (Fig. 5), resulting in $\Delta ED = 11.4$ (± 1.1) ms and $S1–S2_{delay} = 380$ (± 5) ms for the central axis electrodes and $\Delta ED = 19.0$ (± 1.6) ms and $S1–S2_{delay} = 390$ (± 9) ms for the off-axis electrodes.

The LQTS was modeled by first reducing the total conductivity of HERG, responsible for the $I_{Ks}$ current, by 50%, with normal kinetics, in every element. Using a fibrosis-free model, this resulted in curves with a slightly larger increase in delay at the refractory interval, and increases in delay at longer S1–S2 intervals than normal (Fig. 6) but there were no added potentials in the electrogram. Dispersion of refractory periods was modeled as before, by a 50–100% random variation with a rectangular distribution in $I_{Kr}$ density over the entire sheet to simulate variable expression of HERG, which is consistent with reported values for the variation in ventricular effective refractory period (VERP) within the endocardium for patients with the LQTS.[27] This simulation produced greater increases in the number of fractionated potentials with larger increases in electrogram duration than the simulation with reduced $I_{Kr}$ alone. Also, the simulated curves (Fig. 6) are closer to those seen in patients with the LQTS as illustrated by a curve from a patient with LQT2 (i.e., reduction in $I_{Kr}$) and documented VF. The results for a fibrotic sheet with a heart failure AP and dispersion of refractoriness is also compared with results from a DCM VF patient and shows a similar pattern of fractionation. Finally, the imposition of abnormal $Ca^{2+}$ handling resulted in no change in mean ΔED or S1–S2 delay although in one curve there was an attenuation of the most delayed potentials close to VERP (Fig. 7).

## Discussion

This model was developed to understand the basis of an emerging clinical technique that may be useful for the prediction of sudden death. While fractionated electrograms were produced in the model, which appear similar to those seen in patients with heart disease, it is striking that only two simulations gave rise to a reentrant "arrhythmia." This is important in the interpretation of PEFA. A clinical PEFA study is not intended to produce an arrhythmia but to characterize myocardial disease at a limited number of electrode positions. If there are diseased areas detected by PEFA, the conditions for reentry may be present somewhere within the patient's heart and may form the substrate for a lethal arrhythmia. Therefore, a specific substrate may not be detected by PEFA and in these simulations there may be no relationship between reentry and fractionation. One problem in performing clinical investigations is that only a limited number of electrodes can be introduced into the heart and so that the entire myocardium, which may have a potential substrate anywhere, is very sparsely sampled. Nevertheless, HCM, DCM, and LQTS VF patients usually have a number of abnormal areas, implying that they

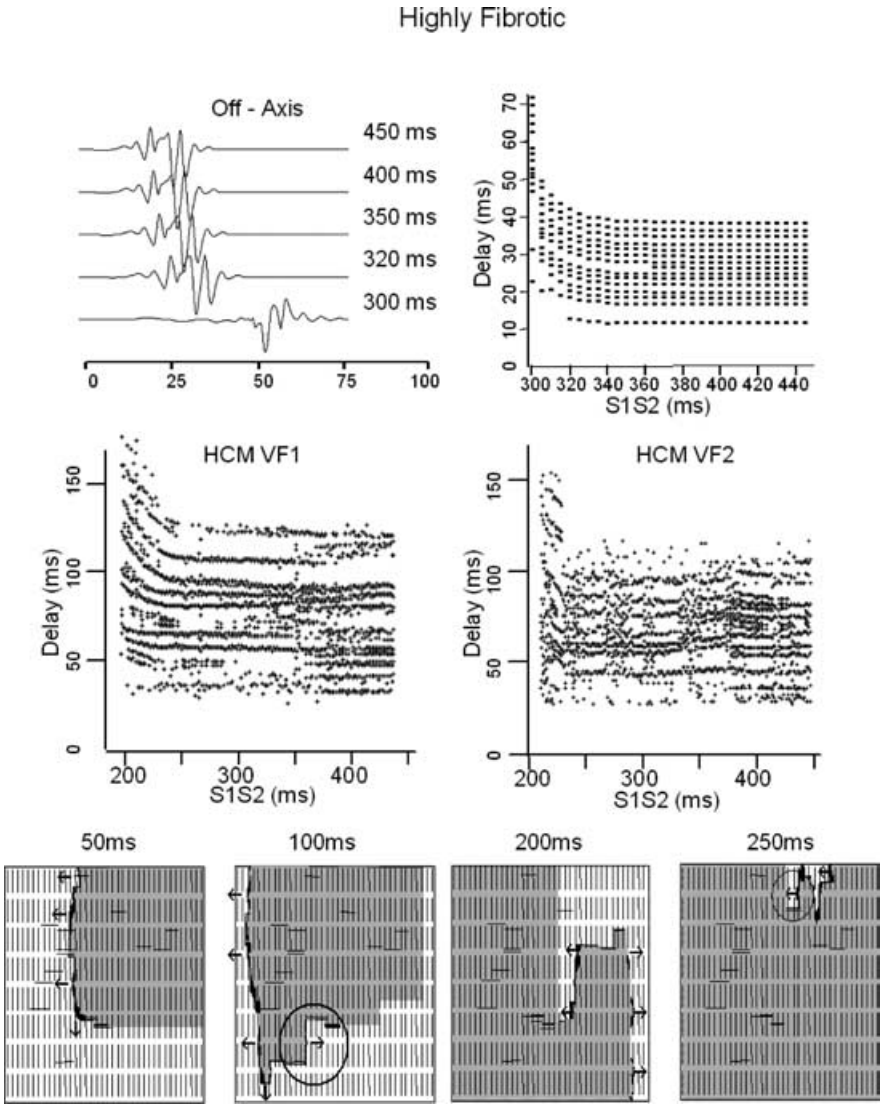


**Figure 4.** *The simulated electrograms for electrodes on and off the central axis are shown at different S1–S2 intervals for highly fibrotic tissue. The corresponding fractionation curves for the simulations are shown and should be compared with those in Figure 3. The lower figures are obtained from HCM VF patients, illustrating the sudden increase in delay at short S1–S2 intervals.*

have widespread disease, and a substrate for VF. Since 19 patients with prospective VF had intense fractionation prior to sudden death or an ICD discharge, PEFA may have a role in risk prediction and ICD implantation in noncoronary disease.

One advantage of a mathematical model is that it allows the contributions of different components of a disease to be studied. The main components in this model are fibrosis and action potential abnormalities and these may be examined independently. Disarray has been modeled by increased transverse fibrosis causing axial block. These effects can be summarized as follows: fibrosis causes fractionation whose

**TABLE 1**

The Change in Electrogram Duration (ΔED) and S1–S2 Interval at Which the Endpoint Increases in Delay ($S1–S2_{Delay}$) for Five Different, Randomly Generated Sheets

| | Central Axis Electrode | | Off-Axis Electrodes | |
|---|---|---|---|---|
| **Tissue Sheet** | **ΔED (ms)** | **$S1–S2_{Delay}$ (ms)** | **ΔED (ms)** | **$S1–S2_{Delay}$ (ms)** |
| No fibrosis | 2.8 | 330 | 3.6 | 330 |
| Minimal fibrosis | 2.6 | 330 | 3.8 | 340 |
| Moderate fibrosis | 2.9 | 330 | 5.6 | 340 |
| Severe fibrosis | 17.2 | 340 | 28.2 | 340 |

The sheets simulate longitudinal fibrosis only.

**TABLE 2**

The Average Change in Electrogram Duration (ΔED) and S1–S2 Interval at Which the Endpoint Increases in Delay ($S1–S2_{Delay}$) for Five Different, Randomly Generated Sheets

| | Central Axis Electrode | | Off-Axis Electrodes | |
|---|---|---|---|---|
| **Tissue Sheet** | **ΔDuration (ms)** | **$S1–S2_{Delay}$ (ms)** | **ΔDuration (ms)** | **$S1–S2_{Delay}$ (ms)** |
| No fibrosis | 2.8 | 330 | 3.6 | 330 |
| Minimal fibrosis | 2.9 (0.3) | 340 (3) | 4.7 (0.9) | 340 (4) |
| Moderate fibrosis | 4.6 (0.7) | 340 (7) | 8.2 (1.4) | 350 (6) |
| Severe fibrosis | 25.6 (3.5) | 360 (8) | 30.2 (6.7) | 360 (10) |

The sheets simulate both longitudinal and transverse fibrosis. The 95% confidence limits are given in parentheses.

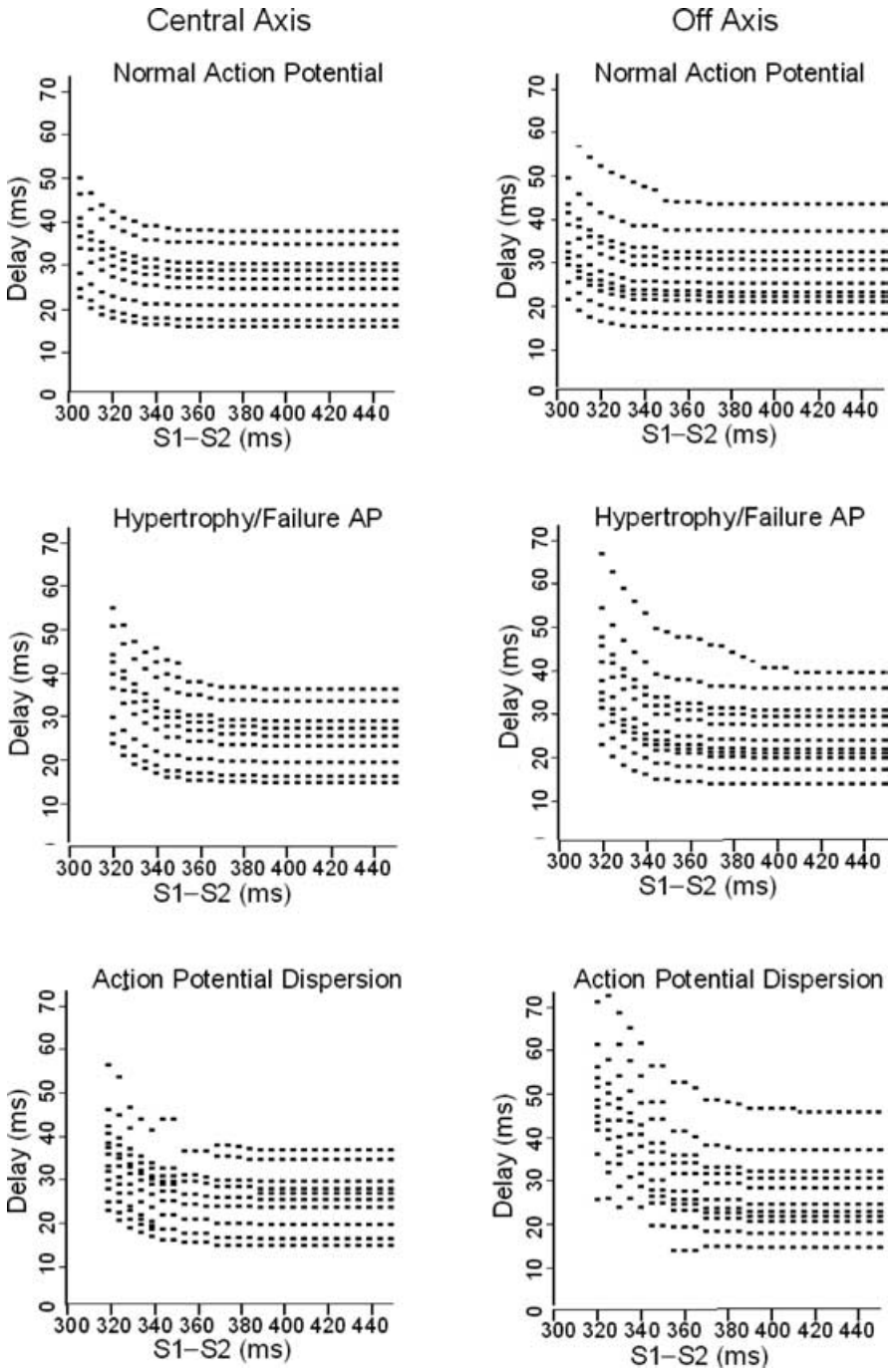


**Figure 5.** *The effects of an abnormal action potential and action potential dispersion on simulated fractionation curves for moderately fibrotic tissue.*

magnitude depends on the density and geometry of the fibrosis. Combined with an abnormal action potential (abnormal calcium handling in the case of HCM and heart failure action potentials) the effects of fibrosis are accentuated by causing functional block and slowed activation because of a longer action potential duration.

### *Mechanisms of Fractionation: The Effects of Fibrosis*

The effect of fibrosis is to block the activation wave front and to cause it to take a circuitous route through the myocardium. The greatest changes in electrogram duration and shape were caused by small gaps (G = 0.5 mm) between lines of fibrous tissue that caused preferential slowing of conduction through these gaps, with functional block occurring at short S1–S2 intervals due to an insufficient $Na^+$ current required to drive the escaping and expanding AP wavefront.[28,29] For the sheet with dense longitudinal fibrosis and a normal AP, the effects of this wavefront curvature caused functional block of transverse propagation and potential reentry following a premature stimulus associated with characteristic prolongation of recorded electrograms. This effect has recently been demonstrated in the highly fibrotic explanted human heart in which propagation across fibrous tissue slows, and may become blocked, while the electrogram becomes prolonged following increasingly

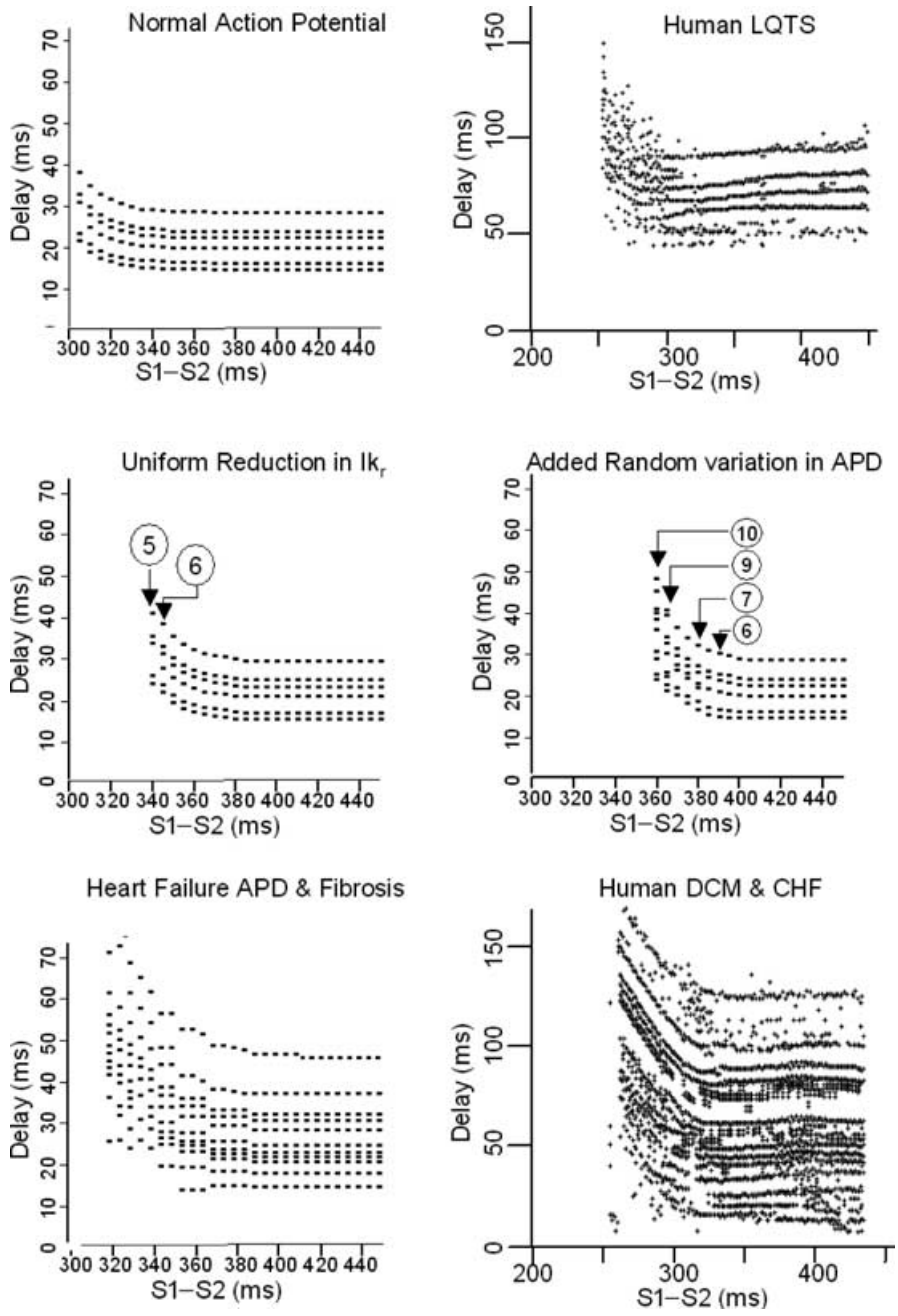


**Figure 6.** *The fractionation curves from a normal control and a patient with LQT2. The simulated results show a normal action potential, the curves when $I_{Kr}$ is reduced uniformly by 50% and the curves when $I_{Kr}$ is reduced and there is a random variation in refractory period. Large changes in electrogram morphology are only seen when there is dispersion of the refractory period. The circled numbers refer to the number of potentials within the electrogram.*

premature stimulation[30] although it seems likely that AP abnormalities would also be present in such severely diseased hearts.

The addition of transverse fibrosis, to mimic disarray in HCM with longitudinal fiber disruption, increased electrogram fractionation by blocking propagation along some paths between longitudinal fibrosis, so increasing the number and complexity of the routes that activity could take through the sheet. With high densities of fibrosis, the interaction between functional blocking of transverse propagation and the complex pattern of fibrosis led to sustained reentry with a variable activation cycle (Fig. 4). The fractionation curve for this case showed increases in duration before induction of reentry that were larger than those seen with other simulations ($\Delta$ED = 64 ms, S1–S2$_{\text{delay}}$ = 390 ms for one of the off-axis electrodes) and is consistent with long ventricular activations when VF is induced during PEFA.[7] or programmed electrical stimulation.[31,32] While this simulation identifies a substrate and reproduces findings seen in a few VF patients, it does not imply that these delays represent a specific arrhythmic substrate in humans as the majority of HCM VF studies does not have this characteristic appearance and, because the recordings are made at a restricted number of sites, they may miss highly abnormal areas but nevertheless still reveal sufficient abnormalities to imply that there is an arrhythmic substrate somewhere in a patient's heart.

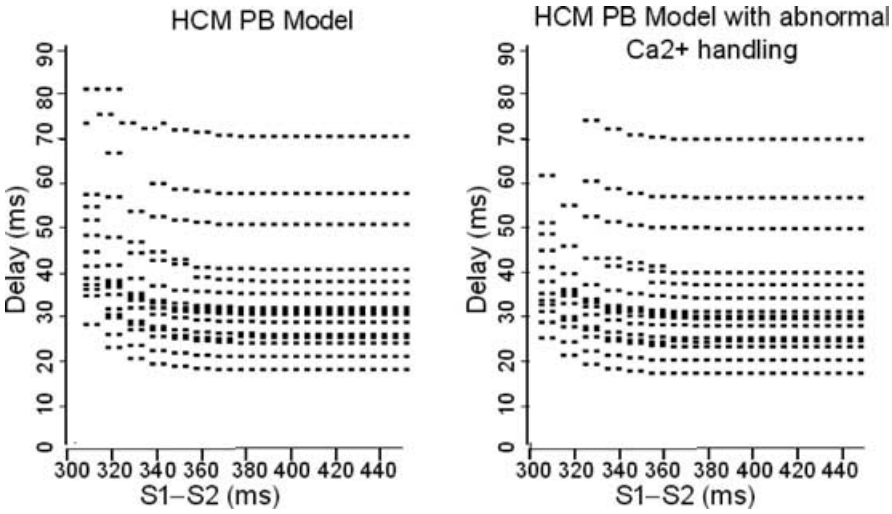


**Figure 7.** *Conduction curves from a maximally fibrotic sheet with normal and abnormal $Ca^{2+}$ handling.*

### *Effects of Action Potential Abnormalities*

Incomplete recovery of the fast inward $Na^+$ current when the extrastimulus is delivered is one possible mechanism of fractionation since, due to its strong voltage dependent gating, this reduces the size of the inward current and results in slower propagation. In the simulation, partial recovery of the $Na^+$ caused the longitudinal velocity (near the pacing electrode) to fall sharply from 0.5 $ms^{-1}$ above an S1–S2 interval of 340 ms to 0.21 $m^{-1}$ at an S1–S2 interval of 305 ms. This effect becomes more significant, however, either in conjunction with structural abnormalities caused by fibrosis or with prolonged repolarization.

The cellular electrophysiological changes seen in hypertrophy and heart failure were simulated using abnormal heart failure APs. These APs caused electrogram prolongation and development of a block at longer S1–S2 intervals than in simulations based on normal APs. This effect, however, depends critically on the shape of AP repolarization phase, as well as its increased duration. The transmembrane voltage restitution, when the cell is reexcited, depends on its rate of repolarization and, on heart failure. This is slower than normal, thus further reducing the size of the fast $Na^+$ activation current and activation velocity, which causes a more gradual increase in electrogram duration with decreasing S1–S2 intervals than would be expected on the basis of the increase

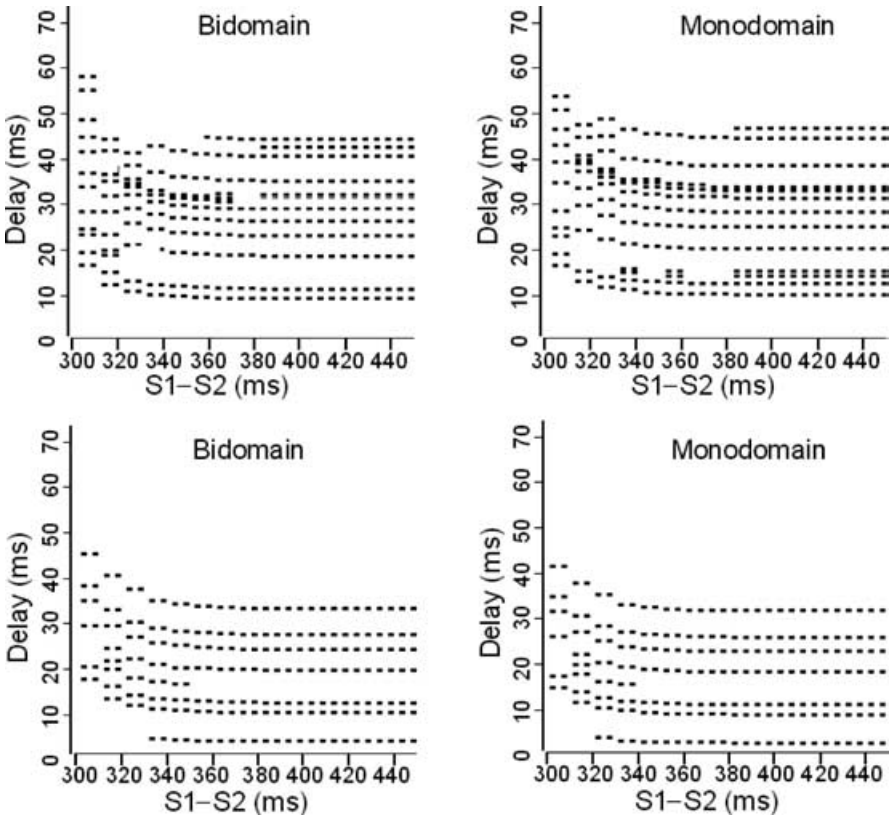


**Figure 8.** *Conduction curves calculated from mono- and bidomain models using the same fibrous sheet and action potential model.*

in APD alone. Hence, using identical sheets, but altering the AP properties, the total increase in electrogram duration was also greater (Fig. 5) although the total reduction in $Na^+$ current is similar in both models. Further increases in the AP duration were created by fibrosis, by removing electrotonic interactions between adjacent areas of cells[14] and causing fractionation of the S2 beat in a similar way to that seen in heart failure (Fig. 6) and this was further increased by modulating the distribution of $I_{Ks}$, and hence APD, over the sheet.

Surprisingly, there is a large degree of fractionation in patients with the LQTS and VF,[10] despite a structurally normal myocardium, and is also seen in the isolated heart when perfused with dofetilide[33] and mice with SCN5A[34] and $I_{Ks}$[35] gene-targeted knockouts. The simulations of LQT2, created by decreasing $I_{Kr}$, showed a small increase in the change in electrogram duration, with the onset occurring at longer S1–S2 intervals than normal (reflecting the longer refractory period) that did not mimic the large increases in fractionation seen in clinical recordings. Increased dispersion of VERP has been reported in the LQTS[27] and this was modeled by the introduction of a random variation in AP duration, again by modulating the $I_{kr}$ distribution over the sheet with a random distribution. This creates areas of functional block due to refractory tissue at short S1–S2 intervals and activation then spreads around them, resulting in fragmentation of the activation wavefront causing increased fractionation (Fig. 6).

Finally, HCM may be associated with abnormal calcium handling. A 30% increase in the $K_d$ of $Ca^{2+}$ to troponin has been described in HCM patients[36] with an $\alpha$ tropomyosin mutation. Also, there is irreversible trapping of $Ca^{2+}$ in the sarcomere of transgenic mice with an $\alpha$-myosin heavy-chain missense mutation that is accompanied by a reduced expression of the ryanodine receptor, phopholamban, and a decrease in calsequestrin content that may lead to a relative increase in cytosolic $Ca^{2+}$, both of which may be stimuli to hypertrophy.[37,38] However, the importance of these effects, in this study, lie in the altered short-term cytosolic $Ca^{2+}$ concentration and hence the membrane potential rather than the long-term shifts between cell compartments that occur with hypertrophy. These effects can be mimicked as troponin $Ca^{2+}$ binding, calsequestrin $Ca^{2+}$ binding, and uptake by the NSR are represented in the PB equations and can be manipulated. Figure 7 shows the results from five different fibrotic models and indicates that PEFA predicts only small changes in the conduction curves calculated with and without abnormal calcium handling. Thus, altered $Ca^{2+}$ homeostasis is unlikely to have a major effect on fractionation in HCM.

### *Limitations of the Model*

These calculations have used a monodomain model in which the effects of extracellular currents are ignored in the model and propagation in diseased myocardium is treated as a continuous medium with discrete obstacles that disturb or block the excitation wavefront. A bidomain model simulates the effects of current flow in extracellular, as well as the intracellular, space, which is known to allow propagation across small obstructions such as capillaries and perimysial collagen. The modification of the initial phase of the AP in bidomain models is well established[39] and since extracellular potentials are generated by current flow in the extracellular domain, they cannot be calculated in monodomain models without simplifying assumptions. Figure 8 shows specimen curves computed from mono- and bidomain models using the same model of fibrosis and AP model. The features are broadly similar although there is a small difference in the delays and activation sequence in curve A and it is likely that discontinuities in propagation are the major determinants of fractionation.

The role of gap junctions has not been considered in this study despite their obvious influence on propagation and local anisotropy in normal tissue. While it is established that there is a reduction of gap junction density associated with fibrosis and that the discontinuities in small-scale propagation are related to gap junction density,[40] the relative contributions of gap junction density, fibrosis, and dispersion of activation to an arrhythmic substrate in diseased myocardium is unknown but may be addressed in future models.

One striking feature of the simulation was that the effective refractory period was longer (280–300 ms) in the model than in humans (220–250 ms) while using the same stimulation sequence. There is evidence that the PB equations do not accurately reflect the dynamic changes in the AP during complex stimulation: in clinical studies with well-defined intracardiac T waves, the measured QT interval shortens more slowly and to a lower ERP than the simulated QT interval using the PB model. The discrepancies between the PB model and actual PEFA results may also be due to the changes in action currents that occur when the cell is not fully repolarized. While this is well understood in the case of the fast $Na^+$ current, the conductivity of HERG has recently been shown to differ following an extrastimulus from that obtained from a single depolarization,[41] which may also be the case for other ion channels and suggests that, for modeling arrhythmias, new formulations of the AP equations will be required.

## Conclusions

The ability of a mathematical model of PEFA to predict some measurements made in patients who are at risk of SCD suggests that its development using large, 3-dimensional models of myocardium incorporating fiber geometry and transmural AP changes will aid understanding of clinical measurements that are related to the risk of lethal arrhythmias. The simulations show that the pattern of fractionation depends on interactions between myocardial fibrosis, AP abnormalities, and dispersion of AP durations. Incorporating all of the abnormalities into the model, each of which can be manipulated individually, resulted in fractionation curves that mimic some features of clinical recordings suggesting that it is feasible to study the relative contributions of individual components of arrhythmic substrates in mathematical models. Nevertheless, the difficulties in making measurements in humans that can distinguish between the different features of the results from such a model are a considerable challenge to clinical electrophysiology.

## References

1. Wu TJ, Ong JJC, Hwang C, Lee JJ, Fishbein MC, Czer L, Trento A, Blanche C, Kass RM, Mandel WJ, Karagueuzian HS, Chen PS: Characteristics of wave fronts during ventricular fibrillation in human hearts with dilated cardiomyopathy: Role of increased fibrosis in the generation of reentry. J Am Coll Cardiol 1998;23:187-196.
2. de Bakker JMT, van Capelle FJL, Janse MJ, Tasseron S, Vermeulen JT, de Jonge N, Lahpor JR: Fractionated electrograms in dilated cardiomyopathy: Origin and relation to abnormal conduction. J Am Coll Cardiol 1996;27:1071-1078.

3. Rogers JM, Huang J, Smith WM, Ideker RE: Incidence, evolution, and spatial distribution of functional reentry during ventricular fibrillation in pigs. Circ Res 1999;84:945-954.
4. Merx W, Yoon MS, Han J: The role of local disparity in conduction and recovery time on ventricular vulnerability to ventricular fibrillation. Am Heart J 1977;94:603-610.
5. Brugada P, Abdollah H, Heddle B, Wellens HJJ: Results of a ventricular fibrillation induced with a single and double ventricular extrastimuli. Am J Cardiol 1983;58:75-79.
6. Bourke JP, Richards DA, Ross DL, McGuire MA, Uther JB: Does the induction of ventricular flutter or fibrillation at electrophysiologic testing after myocardial infarction have any prognostic significance? Am J Cardiol 1995;75:431-435.
7. Saumarez RC, Camm AJ, Panagos A, Gill JS, Stewart JT, de Belder MA, Simpson LA, McKenna WJ: Ventricular fibrillation in hypertrophic cardiomyopathy is associated with increased fractionation of paced right ventricular electrograms. Circulation 1992;86:467-474.
8. Saumarez RC, Slade AKB, Grace AA, Sadoul N, Camm AJ, McKenna WJ: The significance of paced electrogram fractionation in hypertrophic cardiomyopathy. Circulation 1995;91:2762-2768.
9. Saumarez RC, Heald S, Gill J, Slade AKB, de Belder M, Walczak F, Rowland E, Ward DE, Camm AJ: Primary ventricular fibrillation is associated with increased paced right ventricular electrogram fractionation. Circulation 1995;92:2565-2571.
10. Saumarez RC, Chojnowska L, Derksen R, Pytkowski M, Sterlinski M, Huang CL-H, Sadoul N, Hauer RNW, Ruzyo W, Grace AA: Sudden death in noncoronary heart disease is associated with delayed paced ventricular activation. Circulation 2003;107:2595-2600.
11. Roberge FA, Vinet A, Victorri B: Reconstruction of propagated electrical activity with a two-dimensional model of anisotropic heart muscle. Circ Res 1986;58:461-475.
12. Maglaveras N, de Bakker JMT, van Capelle FJL, Pappas C, Janse MJ: Activation delay in healed myocardial infarction: A comparison between model and experiment. Am J Physiol 1995;269:H1441-H1449.
13. Ellis WS, Auslander DM, Lesh MD: Effects of coupling heterogeneity on fractionated electrograms in a model of nonuniformly anisotropic ventricular myocardium. J Electrocardiol. 1997;27:171-178.
14. Lesh MD, Pring M, Spear JF: Cellular uncoupling can unmask dispersion of action potential duration in ventricular myocardium. Circ Res 1989;65:1426-1440.
15. Spach MS, Miller WT, Miller-Jones E, Warren RB, Barr RC: Extracellular potentials related to intracellular action potentials during impulse conduction in anisotropic canine cardiac muscle. Circ Res 1979;45:188-204.
16. Press WH, Teukolsky SA, Vetterling WT, Flannery BP: Numerical recipes in FORTRAN. Cambridge University Press: Cambridge, UK, 1997.
17. Maglaveras N, Sahakian AV, Myers GA: Boundary conditions in simulations of cardiac propagating action potentials. IEEE Trans Biomed Eng 1988;35:755-758.
18. Priebe L, Beuckelmann DJ: Simulation study of cellular electric properties in heart failure. Circ Res 1998;82:1206-1223.
19. Luo CH, Rudy Y: A dynamic model of the cardiac ventricular action potential. Circ Res 1994;74:1071-1096.
20. Coltart DJ, Meldrum SJ: Hypertrophic cardiomyopathy. An electrophysiological study. Br Med J 1970;4:217-218.
21. Hart G: Cellular electrophysiology in cardiac hypertrophy and failure. Cardiovasc Res 1994;28:933-946.
22. Stevenson WG, Weiss JN, Wiener I, Rivitz M, Nademanee K, Klitzner T, Yeatman L, Josephson M, Wohlgelernter D: Fractionated endocardial electrograms are associated with slow conduction in humans: Evidence from pace-mapping. J Am Coll Cardiol 1989;13:369-376.
23. Vechia LL, Ometto R, Bedogni F, Finocchi G, Mosele GM, Bozzola L, Bevilacqua P, Vincenzi M: Ventricular late potentials, interstitial fibrosis and right ventricular function in patients with ventricular tachycardia and normal left ventricular function. Am J Cardiol 1998;81:790-792.
24. Kirchhof JHJ, Josephson ME: Role of discontinuous conduction/nonuniform anisotropy in clinical arrhythmias. In Spooner PM, Joyner RW, Jalife J. eds *Discontinuous Conduction in the Heart*. Futura Publishing, New York, 1997, pp. 135-157.
25. Tanaka M, Fujiwara H, Onodera T, Wu DJ, Matsuda M, Hamashima Y, Kawai C: Pathogenetic role of myocardial fiber disarray in the progression of cardiac fibrosis in normal hearts, hypertensive hearts and hearts with hypertrophic cardiomyopathy. Jpn Circ J 1987 Jun;51:624-630.
26. Varnava AM, Elliott PM, Baboonian C, Davison F, Davies MJ, McKenna WJ: Hypertrophic cardiomyopathy: Histopathological features of sudden death in cardiac troponin T disease. Circulation 2001;104:1380-1384.
27. Vassallo JA, Cassidy DM, Kindwall E, Marchlinski FE, Josephson ME: Nonuniform recovery of the excitability in the left ventricle. Circulation 1988;78:1365-1372.
28. Fast VG, Kleber AG: Block of impulse propagation at an abrupt tissue expansion: Evaluation of the critical strand diameter in 2- and 3-dimensional computer models. Cardiovasc Res 1995;30:449-459.
29. Cabo C, Pertsov AM, Baxter WT, Davidenko JM, Gray RA, Jalife J: Wave-front curvature as a cause of slow conduction and block in isolated cardiac muscle. Circ Res 1994;75:1014-1028.
30. Kawara T, Derksen R, de Groot JR, Coronel R, Tassaeron SRT, Limmenbank AC, Hauer RNW, Kirkels H, Janse MJ, de Bakker JMT: Activation delay after premature stimulation in chronically diseased human myocardium relates to the architecture of interstitial fibrosis. Circulation 2001;104:3069-3075.
31. Avitall B, McKinnie J, Jazayeri M, Akhtar M, Anderson AJ, Tchou P: Induction of ventricular fibrillation versus monomorphic ventricular tachycardia during programmed stimulation. Role of premature beat conduction delay. Circulation 1992;85:1271-1278.
32. Gillis AM, Winkle RA, Echt DS: Role of extrastimulus prematurity and intraventricular conduction time in inducing ventricular tachycardia or fibrillation secondary to coronary artery disease. Am J Cardiol 1987;60:590-595.
33. Saumarez RC and Grace AA: Paced ventricular electrogram fractionation and sudden death in hypertrophic cardiomyopathy and other noncoronary heart diseases. Cardiovascular Res 2000;47:11-22.
34. Papadatos GA, Wallerstein PM, Head CE, Ratcliff R, Brady PA, Benndorf K, Saumarez RC, Trezise AE, Huang CL, Vandenberg JI, Colledge WH, Grace AA: Slowed conduction and ventricular tachycardia after targeted disruption of the cardiac sodium channel gene SCN5A. Proc Natl Acad Sci USA 2002;99:6210-6215.
35. Balasubramaniam R, Grace AA, Saumarez RC, Vandenberg JI, Huang CL-H: Electrogram prolongation and nifedipine-suppressible arrhythmias following targeted disruption of *KCNE1*. J Physiol (Lond) 2003;552:535-546.
36. Karibe A, Tobacman LS, Strand J, Butters C, Back N, Bachinski LL, Arai AE, Ortiz A, Roberts R, Homsher E, Fanapazir L: Hypertrophic Cardiomyopathy caused by a novel $\alpha$ Tropomyosin mutation (V95A) is associated with mild cardiac phenotype, abnormal calcium binding to Troponin, abnormal myosin cycling and poor prognosis. Circulation 2001;103:65-71.
37. Semsarian C, Ahmed I, Giewat M, Georgakopoulos D, Schmitt JP, McKonnell DK, Reiken S, Mende U, Marks AR, Kass DA, Seidman CE, Seidman JG: L –Type calcium channel inhibitor Diltiazem prevents cardiomyopathy in a mouse model. J Clin Invest 2002;109:1013-1020.
38. Fatkin D, McKonnell DK, Mudd JO, Semsarian C, Moskowitz IGP, Schoen FJ, Giewat M, Seidman CE, Seidman JG: An abnormal $Ca^{2+}$ response in mutant sarcomere protein-mediated familial hypertrophic cardiomyopathy. J Clin Invest 2000;106:1351-1359.
39. Spach MS, Barr RC: Effects of cardiac microstructure on propagating electrical waveforms. Circ Res 2000;86:23e-35e.
40. Peters BS, Wit AL: Myocardial Architecture and ventricular arrhythmogensis. Circulation 1998;97:1746-1754.
41. Lu Y, Marhaut-Smith MP, Varghese A, Huang C-L, Kemp PR, Vandenberg JI: Effects of premature stimulation on HERG K+ Channels. J Physiol (Lond) 2001;537:843-851.